The mid-IR spectra of 9-ethyl guanine, guanosine, and 2-deoxyguanosine

Ali Abo-riziq[(a)], Bridgit O. Crews[(a)], Isabelle Compagnon[(b)], Jos Oomens[(b)]; Gerard Meijer[(c)], Gert Von Helden[(c)], Martin Kabeláč[d)], Pavel Hobza[(d)], and Mattanjah S. de Vries[(a)]

(a) Department of Chemistry and Biochemistry, University of California Santa Barbara, CA 93106-9510, USA

(b) FOM-Institute for Plasmaphysics Rijnhuizen, Edisonbaan 14, NL-3439 MN Nieuwegein, The Netherlands

(Electronic address: jmbakker@rijnh.nl)

(c) Fritz-Haber-Institut der Max-Planck-Gesellschaft, Faradayweg 4-6, D-14195 Berlin, Germany

(d) Institute of Organic Chemistry and Biochemistry, Academy of Sciences of the Czech Republic, 166 10 Prague 6 and Center for Complex Molecular Systems and Biomolecules, 166 10 Prague 6, Czech Republic

Abstract

We present the mid-IR (400-1800 cm^{-1}) spectra of 9-ethyl guanine, guanosine, and 2-deoxyguanosine measured by IR-UV double resonance spectroscopy. We compare the recorded mid-IR spectra with the spectra of the most stable structures obtained from RI-MP2 and RI-DFT-D calculations. The results confirm the enol form for all structures and demonstrate the efficacy of a new approach to DFT calculations that includes dispersion interactions.

Introduction

Since our first report of the sharp resonant two-photon ionization (R2PI) spectrum of guanine [1] and guanosine [2] their isomeric structures have commanded considerable scrutiny. In the gas phase under jet cooled conditions, four tautomers of guanine appear based on hole burning spectroscopy [3-7]. Remarkably, it now appears that none of these are in the keto form which is the biologically most relevant type of tautomer because it is the dominant form in solution and it is the form in which Watson-Crick base pairing occurs in DNA [7]. The identification is based on IR-UV hole burning spectroscopy in the near IR range. The OH stretch frequencies serve to clearly identify two of the tautomers as being enol while the other two show no OH stretch at all. However, recent analysis has shown these other two tautomers to be the higher energy oxo-imino tautomers rather than the more stable keto tautomers. Choi and Miller have observed the keto tautomers in helium droplets, showing their IR frequencies to differ from those in the R2PI experiments [8]. Kleinermanns and coworkers have confirmed the oxo-imino assignments for the R2PI case, based on the imino C=N vibrations at about 1680 cm^{-1} [9]. The difference between the R2PI and the helium droplet work is not only in the degree of cooling but also in the detection method [10]. All the R2PI experiments were performed with nanosecond laser pulses and therefore they are blind to species with sub picosecond lifetime excited states. The detection in helium droplets relies on the IR absorption only and does not depend on the excited state characteristics. It is therefore conceivable that the keto tautomers, which are observed exclusively in the droplets, have significantly shorter excited state lifetimes than the other forms. A number of models suggest that the excited state lifetimes in DNA bases are shortened by internal conversion to the ground state, via an intermediate state and mediated by conical intersections [11-18]. It has been proposed that this type of photochemistry is nature's defense mechanism against photochemical damage.

To further focus on the biologically most relevant form we have studied guanine with substituents in the C9 position to mimic the nucleosides, as well as several of the nucleosides themselves [19]. For all of these species we observed only a single isomer

which we determined by near IR-UV hole burning to be of the enol form. We now explore these compounds further by reporting IR-UV holeburning in the mid IR range of 400-1800 cm^{-1}, covering the C=O and the C=N stretch frequencies to confirm absence of both the keto and imino forms and to further explore the fingerprint frequencies for the sugar moiety. We compare both MP2 and DFT-D computations with the experimental data.

Experimental method

We performed the experiment in a previously described laser desorption jet-cooling setup [20-23]. We desorb a mixture of pure compound and some graphite powder from a graphite substrate with pulses from a YAG laser at 1064 nm and less than 1 mJ/pulse. We entrain the desorbed molecules in a pulsed supersonic jet of Ar drive gas. We perform mass selected spectroscopy by resonant two-photon ionization (R2PI), detecting the ions in a linear time-of-flight mass spectrometer. We obtain the IR spectrum by IR-UV hole burning. A few μs before the excitation laser is fired, the IR free electron laser beam interacts with the molecules in the molecular beam. If a vibrational transition is induced by the IR light, molecular population is transferred from the ground state into an excited vibrational state, resulting in a depletion of ground state population. This depletion results in a reduction in the number of ions produced by the UV two photon ionization. By measuring the ion yield of R2PI ions, while varying the wavelength of the IR laser, we obtain an ion-dip spectrum.

The IR radiation is produced at the Free Electron Laser for Infrared eXperiments (FELIX) user facility at the FOM Institute for Plasma Physics in Rijnhuizen, the Netherlands [24]. The temporal output of this 10 Hz, pulsed laser system consists of a 6 μs long burst (macropulse) of micropulses. The micropulse spacing within the burst is set to 1 ns. The spectral bandwidth is adjusted to approximately 0.5% (fwhm) of the central frequency which corresponds to a micropulse duration of about 100 optical cycles. The frequency range that can be covered extends from 40 cm^{-1} to 2000 cm^{-1}, although only the range from 500–2000 cm^{-1} is used in the present study. Typically, energies of up to

100 mJ can be reached in the macropulse. In the present experiment, the UV detection laser is running at a 10 Hz, repetition rate, while FELIX is set to 5 Hz. By independently recording the alternating IR-*on* signal and IR-*off* signal we obtain a normalized ion-dip spectrum that is insensitive to long-term drifts in UV laser power or source conditions.

The high intensity of the IR beam can potentially lead to multiphoton absorption. To assure that our measurements are based on a single photon absorption, we performed the experiment at a number of IR output powers, converted the normalized signal s(ν)into a relative IR absorption cross section σ(ν) using σ(ν) = -log(s(ν)) and corrected for the IR output power in the scanned region.

Theoretical method

We fully optimized the structures of all systems studied by two techniques. a) We employed the resolution of identity (RI-) MP2 level of theory using cc-pVDZ basis set with standard auxiliary basis set. b) We have recently demonstrated the suitability of DFT theory for study of biopolymers, when employed in combination with an empirically treated dispersion term (RI-DFT-D) [25, 26]. For this purpose we employed the TPSS functional [27]. We obtained relative energies and harmonic frequencies at both levels of theory. The numerically calculated harmonic frequencies were scaled by a factor of 0.956 for the RI-MP2 calculations, as used in our previous papers. RI-DFT-D calculated frequencies were not scaled. We used the TURBOMOLE 5.8 program package [28] with implementation of our code for treating the dispersion term.

Results and discussion

Figure 1 shows the tautomeric forms for which we performed the calculations, with the numbering scheme and the nomenclature used in this paper. Figure 2 shows a few of the lowest energy optimized structures. The n3 forms do not occur in the hydrogen bonded guanosines, since those structures only occur for tautomers with no hydrogen in the N3 position.

Table 1 lists relative stabilities in kcal/mol, calculated at the RI-MP2 level, including zero point vibrational energy. The trends and orders of magnitude are reproduced equally by RI-MP2 and RI-DFT-D methods. The keto and enol structures are always lowest in energy, with a difference of less than 1.5 kcal/mol. The next highest energy structures are the n3 structures (1H,3H imino-oxo) by 12-17 kcal/mol. All other structures are considerably higher in energy. The *cis* form of the guanosines (stabilized by a hydrogen bond between the N3 on the guanine and the C5'-OH on the sugar) is consistently lower in energy than the extended *trans* form by 6-8 kcal/mol. Table 2 lists total electronic energies of the keto tautomers calculated at the RI-DFT-D and RI-MP2 levels.

Figure 3 shows the R2PI spectra of 9-ethyl guanine (a), guanosine (b), and 2-deoxyguanosine (c) scanned in the region of 34400-35400 cm^{-1}. According to the UV-UV double resonance spectroscopy these spectra reflect absorption by only a single isomer. Based on our IR-UV double resonance spectroscopy in the region of 3200-3800 cm^{-1}, we assigned the structure of this isomer in each of the three compounds as the enol form [19]. This assignment is consistent with the R2PI spectroscopy of the guanine nucleobase, for which the 9H enol tautomer has its origin at 34755 cm^{-1}, as compared to the guanosine origin at 34443 cm^{-1} [2, 7]. The two guanine tautomers that have no free OH stretch frequency in the IR-UV spectra have their origins at 32864 cm^{-1} and 33269 cm^{-1}, respectively[4]. We scanned down to 30000 cm^{-1} with two color ionization without finding any additional peaks. As the second color we used both 266 nm and 193 nm to ensure that we would not miss any excitation due to a high ionization potential.

The keto tautomers are missing in the R2PI spectra in all cases. In unsubstituted guanine three additional low energy tautomers exist that each have the N7H rather than the N9H form, and thus have no equivalent form with the 9 substituted compounds. These are the N7H enol, at approximately 4.5 kcal/mol and the two N7H imino-oxo tautomers at approximately 7 kcal/mol, corresponding to A, B, and C respectively in earlier R2PI assignments [7]. The N9H imino-oxo tautomers of guanine are at considerably higher energies of 15-17 kcal/mol, comparable to the corresponding tautomers in the 9

substituted compounds listed in table 1. The near IR-UV data also establish the guanosines to be of the intramolecularly hydrogen bonded *cis* form, based on the absence of the free C'5-O-H stretch.

IR-UV double resonance spectra

Figure 4 shows the IR-UV double resonance spectra of guanosine (a), 2-deoxyguanosine (b), and 9-ethyl guanine (c). For an initial analysis it is useful to compare spectra of structurally related molecules while a more complete analysis requires comparison with ab initio computations. By comparing the IR-UV double resonance spectra of the guanosines with that of 9-ethyl guanine, we can distinguish ring modes *vs.* sugar modes. By comparing the spectra of guanosine and 2-deoxyguanosine, we may distinguish contributions of hydroxyls in the 2^{nd} and 3^{rd} position on the sugar ring. The peaks marked in red appear in all three spectra and belong to guanine ring modes that are common to each molecule. The peaks marked in green in trace (a) are associated with C'2-OH modes that are absent in 2-deoxyguanosine, trace (b). The remaining peaks are due to the substituent or to combination modes involving the substituent.

Figures 5-7 show the IR-UV double resonance spectra compared to calculated frequencies of the various structures. Comparison of the calculated frequencies of each structure with the experimental IR spectra shows the enol form to be the best match for each of the three compounds for several reasons. Most notably, the C=O stretch mode, which we calculated at about 1745 cm^{-1} for the keto form, does not appear in the experimental spectra. Furthermore, those forms would show a single strong peak in the range of 1600-1650 cm^{-1}, due to the C=NH stretch for the imino form, or a symmetric NH_2 bend for the keto form. By contrast the enol form has three strong modes of roughly equal intensity, within a range of about 1600-1650 cm^{-1}. These are the OH bending associated with the C=C stretching of the ring, the C=C stretching and the NH_2 symmetric bending. Furthermore, we see a strong set of peaks at about 1275 cm^{-1}, which we attribute to a strong in-plane OH bending mode, and at about 1425 cm^{-1}, which we attribute to a ring pinching mode of the guanine. Both these strong modes are absent in

the two keto forms. The only other strong guanine mode would be an NH bending vibration for the imino form at about 1100 cm^{1}, which we do not observe.

9-ethyl guanine

Figure 5 shows the experimental IR-UV double resonance spectrum (top trace). The stick spectra represent the DFT-D frequencies of the three lowest energy structures (traces b-d) and the MP2 frequencies for the enol form, for comparison (trace e). Several peaks in the 9-ethylguanine IR-UV double resonance spectrum are absent in the corresponding spectra for guanosine and 2-deoxyguanosine. We note in particular the peaks appearing at 1444 cm^{-1}, 1363 cm^{-1}, and 957 cm^{-1}. We assign the first peak as the CH_2 symmetric bending of the ethyl group, the second peak as the CH_3 umbrella stretch, and the third peak as the C-C stretching mode of the ethyl. The calculations predict these peaks at 1433 cm^{-1}, 1339 cm^{-1}, and 988 cm^{-1} respectively, however their intensity is not reproduced properly by the computations at either the MP2 or the DFT level. Overall the enol form exhibits the best fit, with a better fit for the DFT-D method than for the MP2 method.

Guanosine

Figure 6 shows the experimental IR-UV double resonance spectrum (top trace). The stick spectra represent the frequencies of the five lowest energy structures: The hydrogen bonded (b) and extended (c) enol forms, the hydrogen bonded keto (e), extended 3a (f) and hydrogen bonded 1b form (g). We also show the MP2 results for the hydrogen bonded enol structure in trace (d).

Similarly to 9-ethyl guanine, we can exclude all of the keto forms as possible structures, consistent with the near IR results. The spectra in traces (b) and (c) are very similar with as the main difference a medium-intensity peaks at 948 and at 1501 cm^{-1} in (b), marked in blue, that are absent in (c). These peaks belong to modes of the hydrogen bonded C'5-OH of the sugar. Their modest intensity precludes a very confident assignment with experimental data, however the earlier near IR data strongly suggest the hydrogen bonded

form. We associate the two peaks marked in green with C'2-OH modes. This assignment is consistent with the 2-deoxyguanosine results, presented in Figure 7.

The remaining peaks involve the sugar modes, most of which are much more difficult to assign due to the coupling between different modes and less confident predictions of the calculations in the region below 1000 cm^{-1}.

2-deoxyguanosine

Figure 7 shows the IR-UV double resonance spectrum of 2-deoxyguanosine in trace (a). Trace (b-d) show calculated frequencies for the hydrogen bonded enol form. Panels (b) and (c) compare between guanosine and 2-deoxyguanosine, and panels (b) and (d) compare between results from DFT-D and MP2 methods.

The only difference between guanosine and 2-deoxyguanosine is that the OH in the C'2 position of the sugar is replaced by a hydrogen atom. Therefore, we should expect the disappearance of the peak which we assigned in guanosine to the C'2-OH modes. Because of the overlap with the C-N stretching mode of the guanine ring, we still see a peak at about 1500 cm^{-1} which however is much narrower in comparison to that in guanosine. The sugar ring modes in the region of 1041-1134 cm^{-1}differ between the two spectra however the analysis is hampered by strong coupling.

Summary

Most of the structural studies of biomolecules in the gas phase so far are determined by spectroscopy in the IR range of 3000-4000 cm^{-1} where it is possible to measure the OH, NH, and NH_2 symmetric and antisymmetric modes. This region is very sensitive to structural changes. The mid IR region of 500-2000 cm^{-1} usually contains a complicated series of absorptions (e.g. bending vibrations) and is more difficult to analyze. Widely tunable mid-IR sources are not readily available and much less research is done in this region as a result. However, subtle structural information, such as side chain

conformations, is in principle encoded in the spectra at these wavelengths. Furthermore this region is important because it can provide a valuable test of theoretical calculations.

We obtained the IR absorption spectrum of 9-ethyl guanine, guanosine, and 2-deoxyguanosine isolated in the gas phase in the mid-IR region, between 450 cm^{-1} and 1800 cm^{-1}. These spectra contain a large number of sharp resonances that can be used for structural assignment by comparison with the theoretical spectra of a set of possible geometries. Calculations show that the keto hydrogen bonded conformers of guanosine, 2-deoxyguanosine, and the keto form of 9-ethyl guanine are the most stable structure, as is the keto form of unsubstituted guanine. However, it appears that we observe neither the oxo-imino form, which is observed for guanine, nor the keto form, which is absent in guanine also. Helium droplet data, obtained by Roger Miller and co-workers, show that the keto form of guanine can exist in the gas phase. It is therefore plausible that the fact that we do not observe the keto form for any of the guanosines in R2PI experiments is due to a tautomer selective short excited state lifetime.

The sugar modes are well resolved and add information to the earlier data from the near IR, but they continue to pose an important challenge for further refinement of theoretical computations. This low frequency range serves as a stringent test of computational methods. Judging by the most prominent lines, such as those around 1600 cm^{-1}, it appears that the novel DFT-D approach provides promising agreement with experiment, superior to that resulting from the MP2 approach.

Acknowledgment

We gratefully acknowledge the support by the *Stichting voor Fundamenteel Onderzoek der Materie* (FOM) in providing the required beam time on FELIX and highly appreciate the skillful assistance by the FELIX staff. This material is based upon work supported by the National Science Foundation under Grant No. CHE-0615401. MK and PH acknowledge the support *by Grants Nos. LC512 (from the Ministry of Education of the Czech Republic), 203/05/009 (from the Grant Agency of the Czech Republic).*

References

[1] E. Nir, L. I. Grace, B. Brauer, and M. S. de Vries, "REMPI Spectroscopy of Jet Cooled Guanine," *Journal of the American Chemical Society,* vol. 121, pp. 4896-4897, 1999.

[2] E. Nir, P. Imhof, K. Kleinermanns, and M. S. de Vries, "REMPI spectroscopy of laser desorbed guanosines," *Journal of the American Chemical Society,* vol. 122, pp. 8091-8092, AUG 23 2000.

[3] F. Piuzzi, M. Mons, I. Dimicoli, B. Tardivel, and Q. Zhao, "Ultraviolet spectroscopy and tautomerism of the DNA base guanine and its hydrate formed in a supersonic jet," *Chemical Physics,* vol. 270, pp. 205-14, 2001.

[4] M. Mons, I. Dimicoli, F. Piuzzi, B. Tardivel, and M. Elhanine, "Tautomerism of the DNA base guanine and its methylated derivatives as studied by gas-phase infrared and ultraviolet spectroscopy," *Journal of Physical Chemistry A,* vol. 106, pp. 5088-5094, MAY 23 2002.

[5] W. Chin, M. Mons, I. Dimicoli, F. Piuzzi, B. Tardivel, and M. Elhanine, "Tautomer contribution's to the near UV spectrum of guanine: towards a refined picture for the spectroscopy of purine molecules," *European Physical Journal D,* vol. 20, pp. 347-355, SEP 2002.

[6] W. Chin, M. Mons, F. Piuzzi, B. Tardivel, I. Dimicoli, L. Gorb, and J. Leszczynski, "Gas phase rotamers of the nucleobase 9-methylguanine enol and its monohydrate: Optical spectroscopy and quantum mechanical calculations," *Journal of Physical Chemistry A,* vol. 108, pp. 8237-8243, OCT 7 2004.

[7] M. Mons, F. Piuzzi, I. Dimicoli, L. Gorb, and J. Leszczynski, "Near-UV resonant two-photon ionization spectroscopy of gas phase guanine: Evidence for the observation of three rare tautomers," *Journal of Physical Chemistry A,* vol. 110, pp. 10921-10924, Sep 28 2006.

[8] M. Y. Choi and R. E. Miller, "Four tautomers of isolated guanine from infrared laser spectroscopy in helium nanodroplets," *Journal of the American Chemical Society,* vol. 128, pp. 7320-7328, Jun 7 2006.

[9] K. Kleinermanns, *Private communication,* 2006.

[10] M. Y. Choi, G. E. Douberly, T. M. Falconer, W. K. Lewis, C. M. Lindsay, J. M. Merritt, P. L. Stiles, and R. E. Miller, "Infrared spectroscopy of helium nanodroplets: novel methods for physics and chemistry," *International Reviews in Physical Chemistry,* vol. 25, pp. 15-75, Jan-Jun 2006.

[11] A. Broo and A. Holmen, "Ab initio MP2 and DFT calculations of geometry and solution tautomerism of purine and some purine derivatives," *Chem. Phys.,* vol. 211, pp. 147-161, 1996.

[12] A. L. Sobolewski and W. Domcke, "On the mechanism of nonradiative decay of DNA bases: ab initio and TDDFT results for the excited states of 9H-adenine," *European Physical Journal D,* vol. 20, pp. 369-374, SEP 2002.

[13] T. Schultz, E. Samoylova, W. Radloff, I. V. Hertel, A. L. Sobolewski, and W. Domcke, "Efficient deactivation of a model base pair via excited-state hydrogen transfer," *Science,* vol. 306, pp. 1765-1768, DEC 3 2004.

[14] A. L. Sobolewski and W. Domcke, "Relevance of electron-driven proton-transfer processes for the photostability of proteins," *Chemphyschem,* vol. 7, pp. 561-564, Mar 13 2006.
[15] H. Kang, B. Jung, and S. K. Kim, "Mechanism for ultrafast internal conversion of adenine," *Journal of Chemical Physics,* vol. 118, pp. 6717-6719, APR 15 2003.
[16] C. Canuel, M. Mons, F. Piuzzi, B. Tardivel, I. Dimicoli, and M. Elhanine, "Excited states dynamics of DNA and RNA bases: Characterization of a stepwise deactivation pathway in the gas phase," *Journal of Chemical Physics,* vol. 122, p. 7, FEB 15 2005.
[17] C. M. Marian, "A new pathway for the rapid decay of electronically excited adenine," *Journal of Chemical Physics,* vol. 122, p. 10, Mar 8 2005.
[18] E. Nir, K. Kleinermanns, L. Grace, and M. S. de Vries, "On the photochemistry of purine nucleobases," *Journal of Physical Chemistry A,* vol. 105, pp. 5106-5110, MAY 31 2001.
[19] E. Nir, I. Hunig, K. Kleinermanns, and M. S. de Vries, "Conformers of guanosines and their vibrations in the electronic ground and excited states, as revealed by double-resonance spectroscopy and ab initio calculations," *Chemphyschem,* vol. 5, pp. 131-137, JAN 23 2004.
[20] J. M. Bakker, L. Mac Aleese, G. von Helden, and G. Meijer, *Physical Review Letters,* vol. in press, 2003.
[21] J. M. Bakker, R. G. Satink, G. von Helden, and G. Meijer, "Infrared photodissociation spectroscopy of benzene-Ne,Ar complex cations," *Physical Chemistry Chemical Physics,* vol. 4, pp. 24-33, 2002.
[22] G. Meijer, M. S. Devries, H. E. Hunziker, and H. R. Wendt, "Laser Desorption Jet-Cooling of Organic-Molecules - Cooling Characteristics and Detection Sensitivity," *Applied Physics B-Photophysics and Laser Chemistry,* vol. 51, pp. 395-403, DEC 1990.
[23] J. M. Bakker, L. M. Aleese, G. Meijer, and G. von Helden, "Fingerprint IR spectroscopy to probe amino acid conformations in the gas phase," *Physical Review Letters,* vol. 91, pp. -, NOV 14 2003.
[24] D. Oepts, A. F. G. van der Meer, and P. W. van Amersfoort, "The Free-Electron-Laser User Facility Felix," *Infrared Physics & Technology,* vol. 36, pp. 297-308, JAN 1995.
[25] P. Jurečka, J. Černy, P. Hobza, and D. R. Salahub, "Density functional theory augmented with an empirical dispersion term. Interaction energies and geometries of 80 noncovalent complexes compared with ab initio quantum mechanics calculations," *Journal of Computational Chemistry,* vol. 28, pp. 555-569, 2007.
[26] P. Jurečka, J. Černý, P. Hobza, and H. Valdés, *Journal of Physical Chemistry A,* vol. 111, pp. 1146-1154, 2007.
[27] J. M. Tao, J. P. Perdew, V. N. Staroverov, and G. E. Scuseria, "Climbing the density functional ladder: Nonempirical meta-generalized gradient approximation designed for molecules and solids," *Physical Review Letters,* vol. 91, p. 146401, Oct 3 2003.
[28] R. Ahlrichs, M. Bär, M. Häser, H. Horn, and C. Kölmel, "Electronic-Structure Calculations on Workstation Computers - the Program System Turbomole," *Chemical Physics Letters,* vol. 162, pp. 165-169, OCT 13 1989.

Figure captions

Figure 1. Tautomeric forms of 9-substituted guanines.

Figure 2. The lowest-energy structures of 9-ethyl guanine, guanosine, and 2-deoxyguanosine.

Figure 3. R2PI spectra of 9-ethyl guanine (a), 2-deoxyguanosine (b), and guanosine (c), scanned in the region 34400-35400 cm-1. Based on UV-UV double resonance (not shown) for each molecule, all the peaks in this region belong to one conformation.

Figure 4. The mid-IR spectra in the region (480-1800 cm-1) of guanosine (a), 2-deoxyguanosine (b), and 9-ethyl guanine (c). Red peaks are due to modes of the guanine chromophore; green peaks indicate C'2-OH modes.

Figure 5. The experimental mid-IR spectrum of 9-ethyl guanine (top panel) and the calculated frequencies of the lowest energy structures.

Figure 6. The experimental mid-IR spectrum of guanosine (top panel) and the calculated frequencies of the lowest energy structures

Figure 7. The experimental mid-IR spectrum of 2-deoxyguanosine (top panel) and the calculated frequencies of the lowest energy structures. The guanosine calculation (third trace) is shown for comparison.

Table 1: Relative stabilities (kcal/mol), calculated at the RI-MP2 level, including zero point vibrational energy.

Structure	guanine	ethyl guanine	guanosine extended	guanosine H-bonded	deoxy guanosine extended	deoxy guanosine H-bonded
keto	0.00	0.00	0.00	-6.91	0.00	-6.83
enol	1.49	1.40	1.38	-6.16	1.13	-5.91
ia	36.24	33.02	32.97	23.19	31.89	24.57
ib	30.64	27.67	27.29	18.34	26.63	19.58
n3a	15.62	15.32	11.96		15.04	
n3b	17.30	16.92	13.00		16.45	
oh1a	32.57	31.24	30.97	22.61	30.86	23.71
oh1b	25.74	24.54	24.06	16.12	24.11	17.09
oh2a	39.83	38.58	38.32	30.31	38.23	31.37
oh2b	32.26	31.12	30.59	22.97	30.77	23.88

Table 2: Comparison of total energies (E_h) calculated with RI-MP2 and RI-DFT-D methods.

Structure (method)	guanine	ethyl guanine	guanosine extended	guanosine H-bonded	deoxy guanosine extended	deoxy guanosine H-bonded
keto (DFT-D)	-542.8	-621.5	-1039.3	-1039.3	-964.0	-964.0
keto (MP2)	-539.4	-617.5	-1032.9	-1032.9	-958.0	-958.0

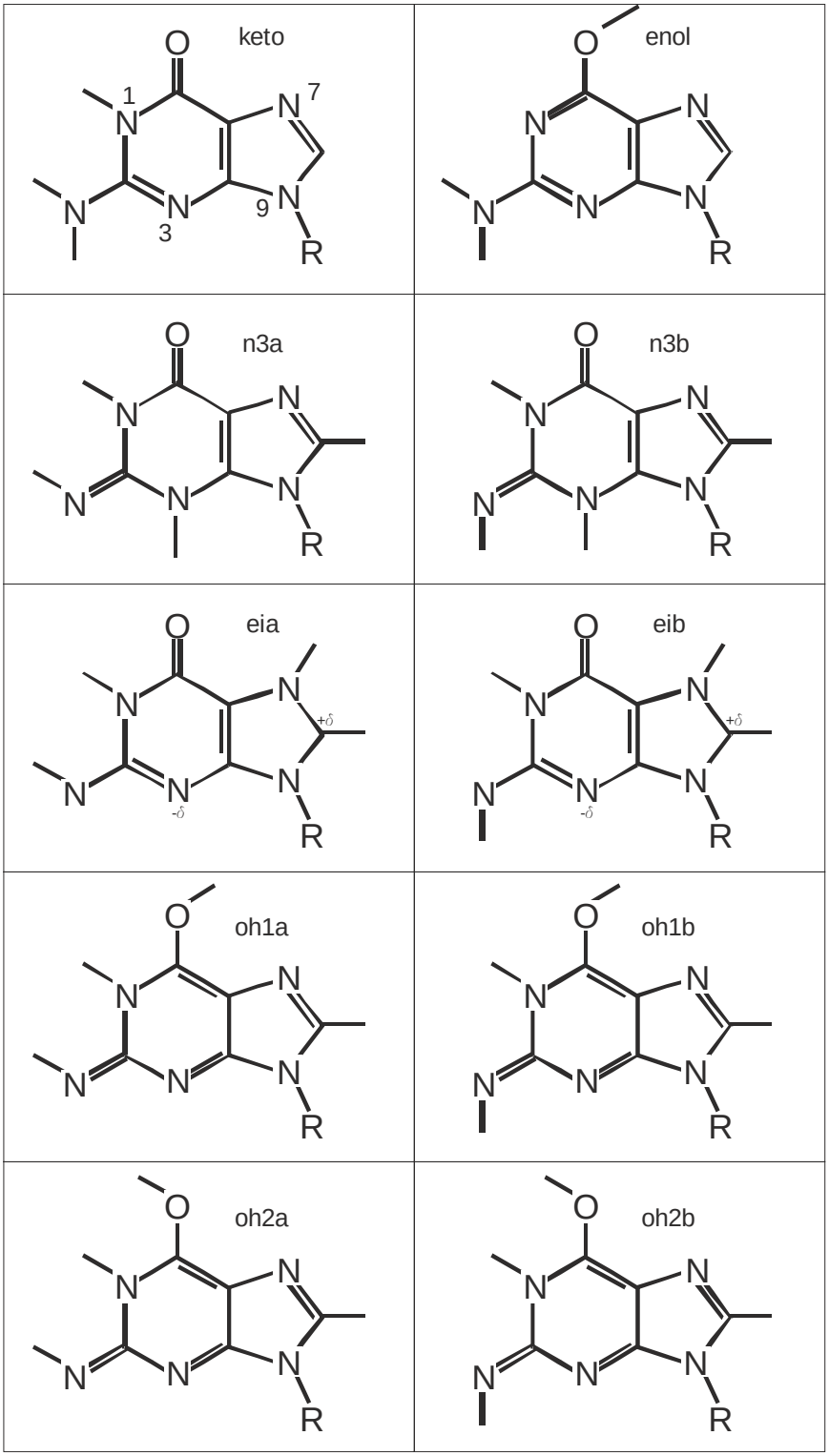

Figure 1

9-Ethyl guanine

Enol	Keto
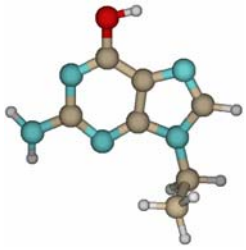	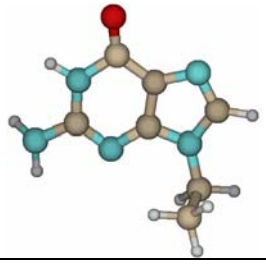

Guanosine

Enol (HB)	Enol (extended)	Keto (HB)	Keto (Extended)
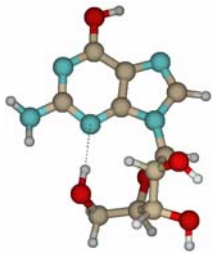	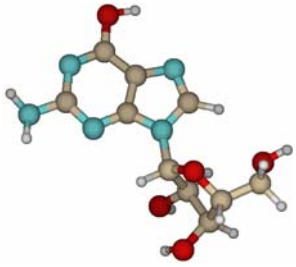	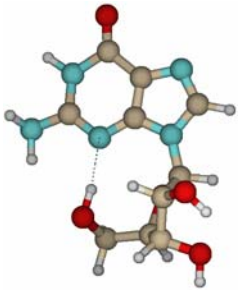	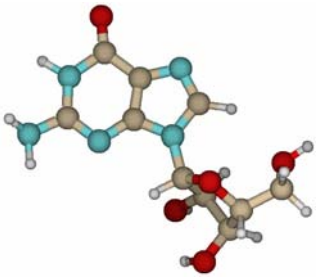

2-Deoxyguanosine

Enol (HB)	Enol (extended)	Keto (HB)	Keto (Extended)
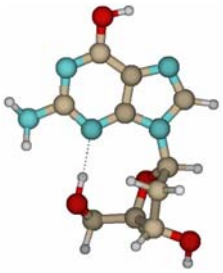	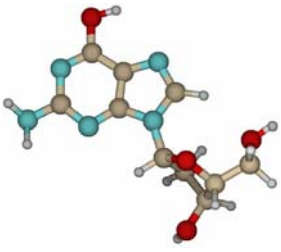	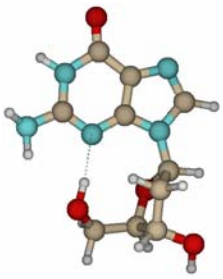	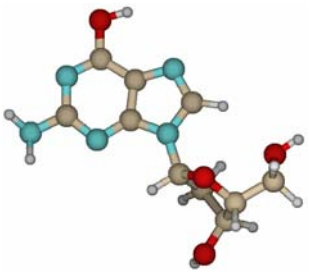

Figure 2

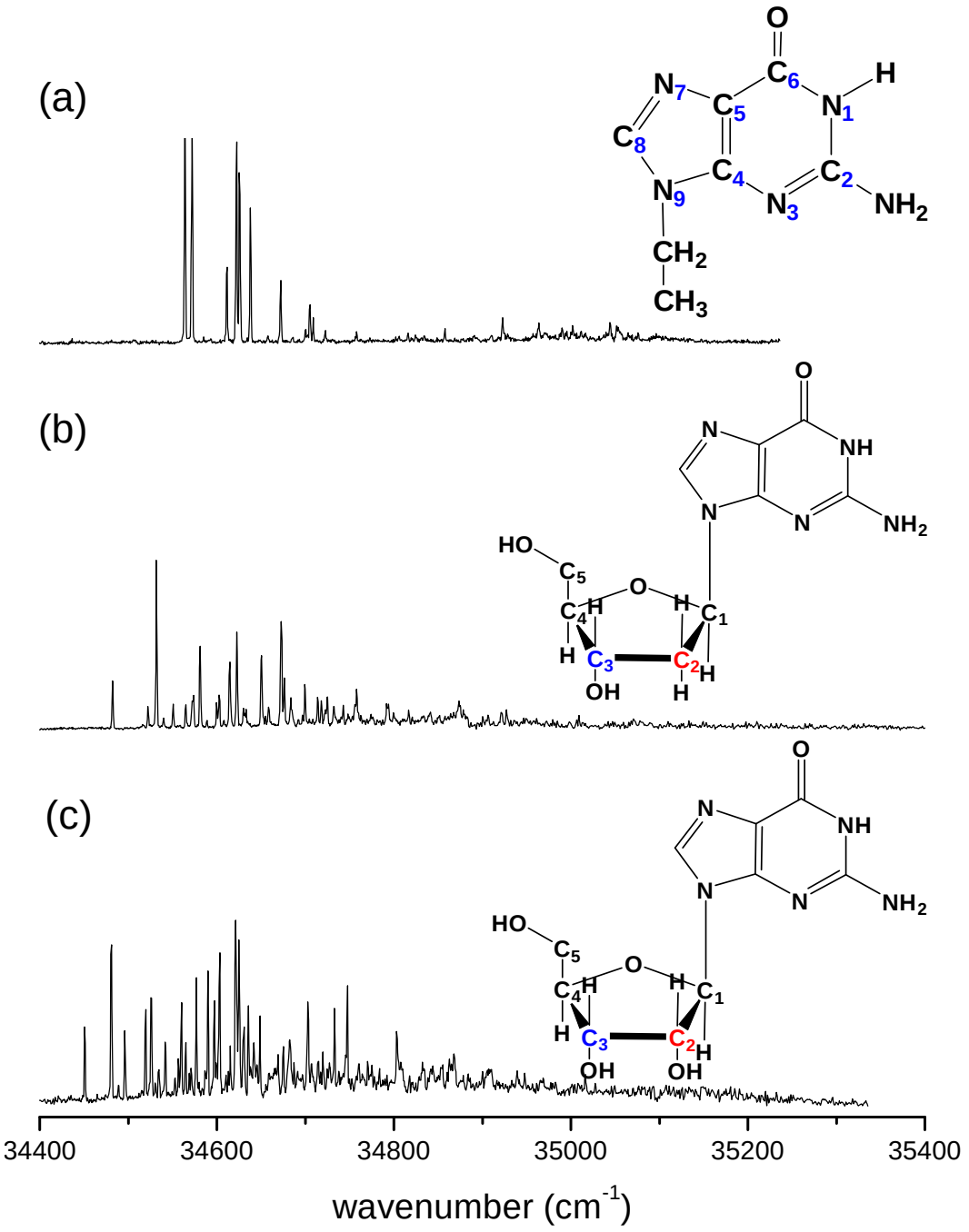

Figure 3

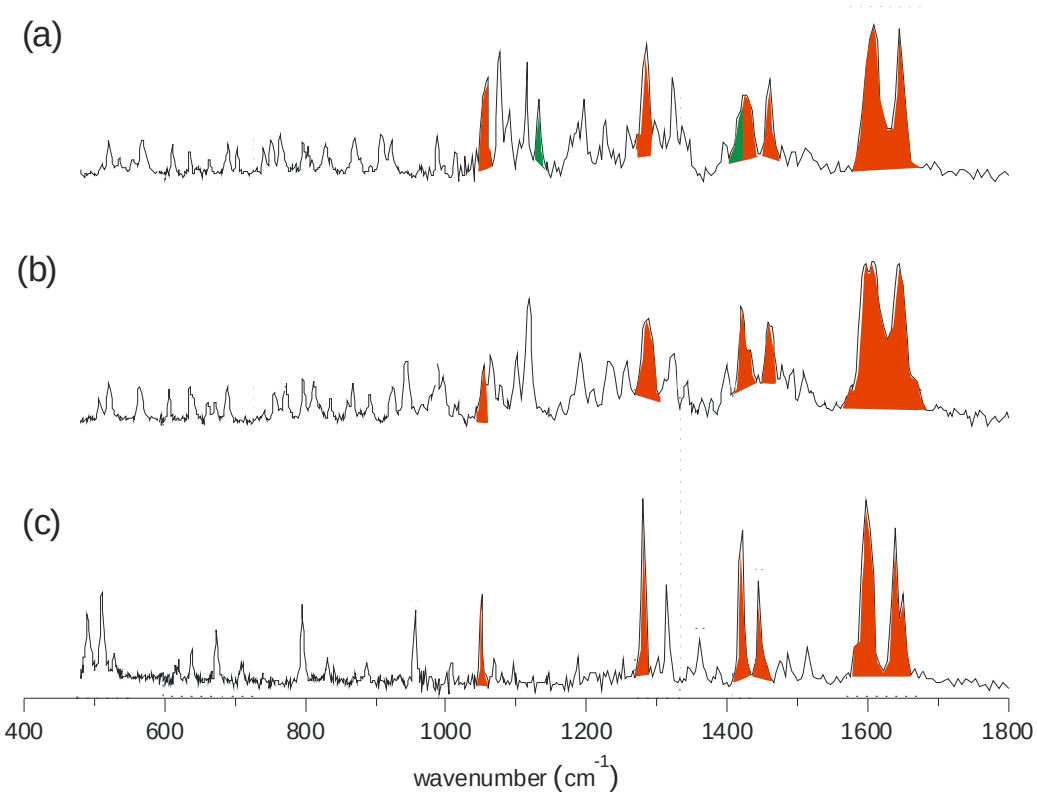

Figure 4

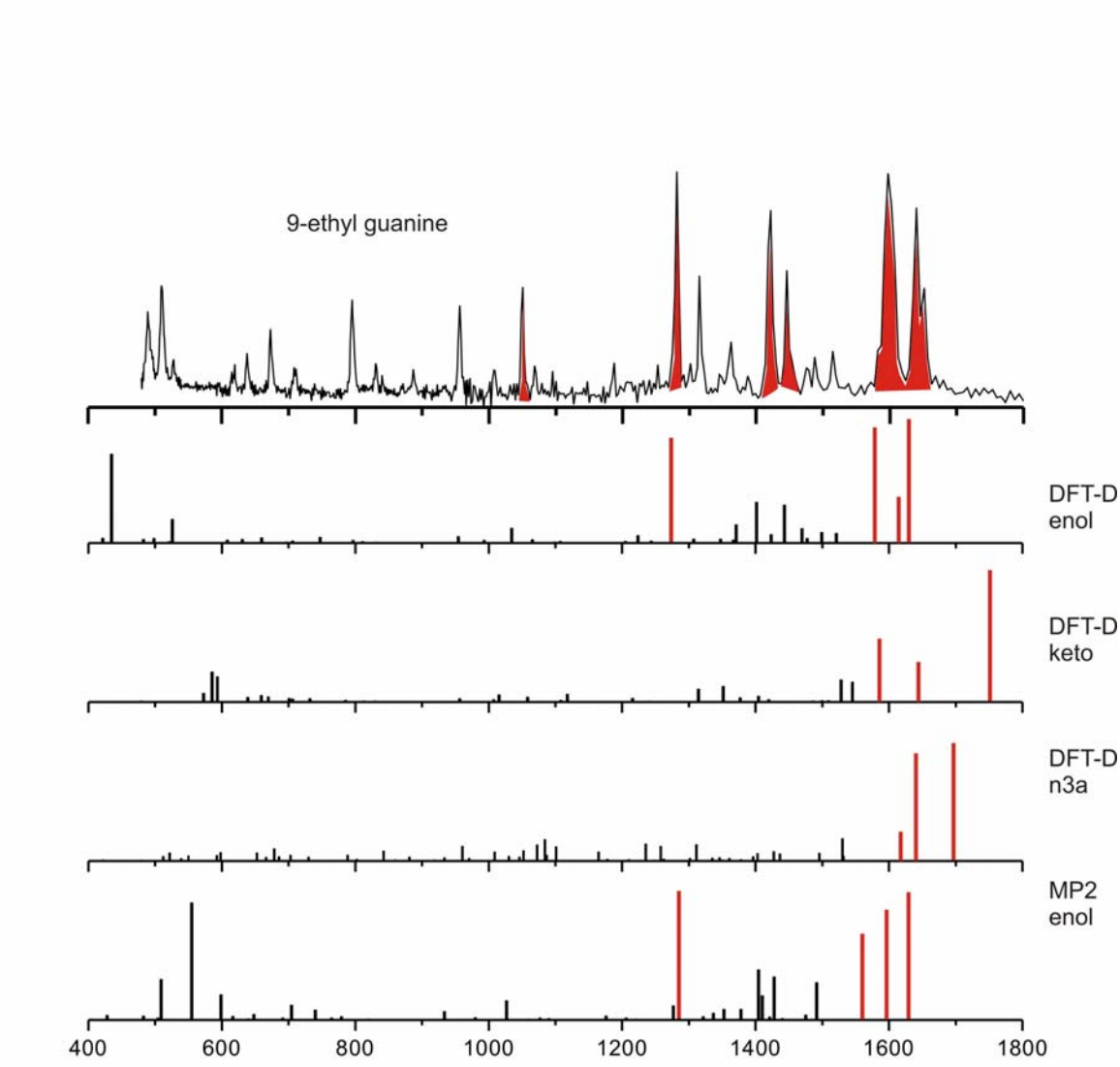
9-ethyl guanine
DFT-D
enol
DFT-D
keto
DFT-D
n3a
MP2
enol
400
600
800
1000
1200
1400
1600
1800

Figure 5

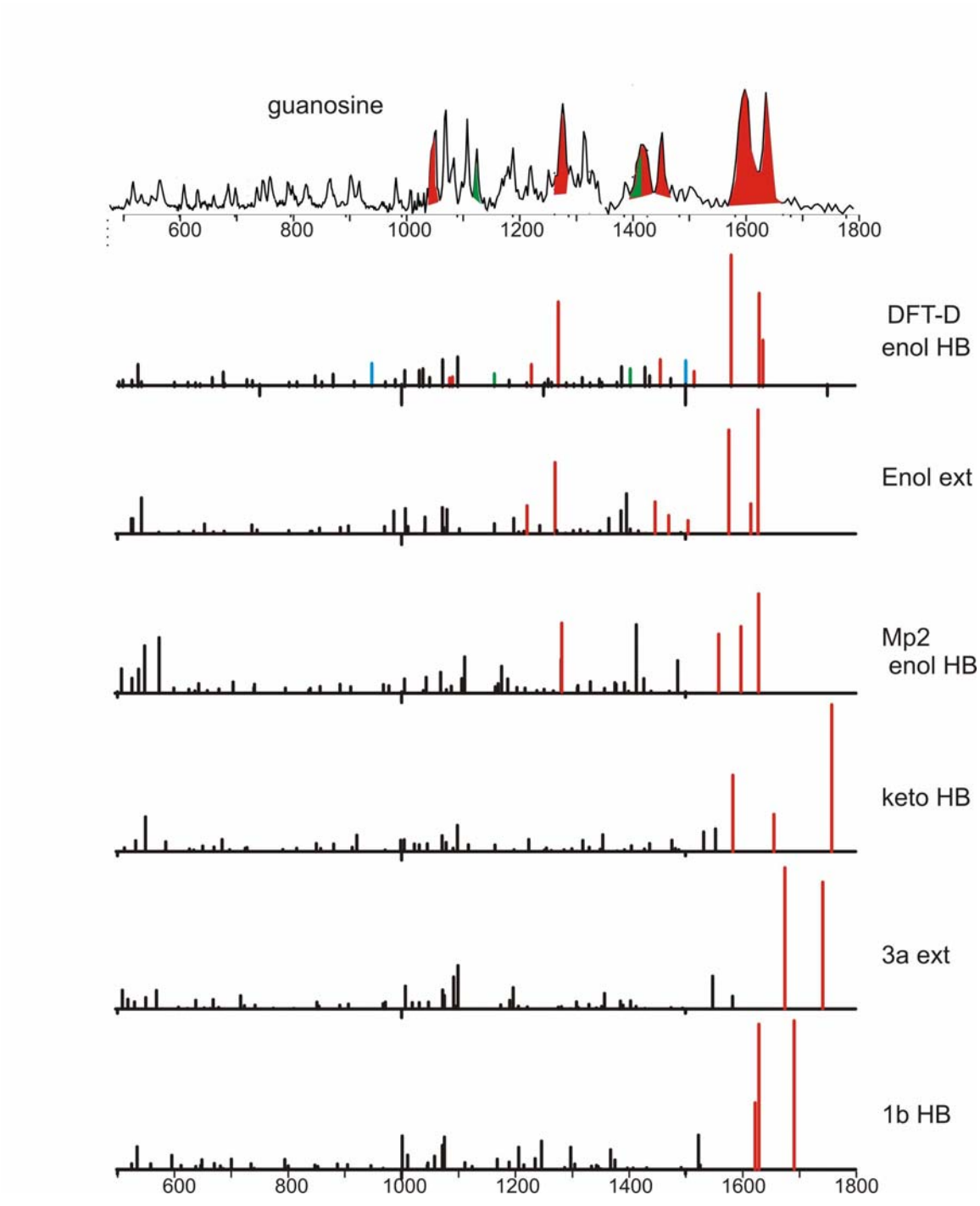
guanosine
600
800
1000
1200
1400
1600
1800
DFT-D
enol HB
Enol ext
Mp2
enol HB
keto HB
3a ext
1b HB
600
800
1000
1200
1400
1600
1800

Figure 6

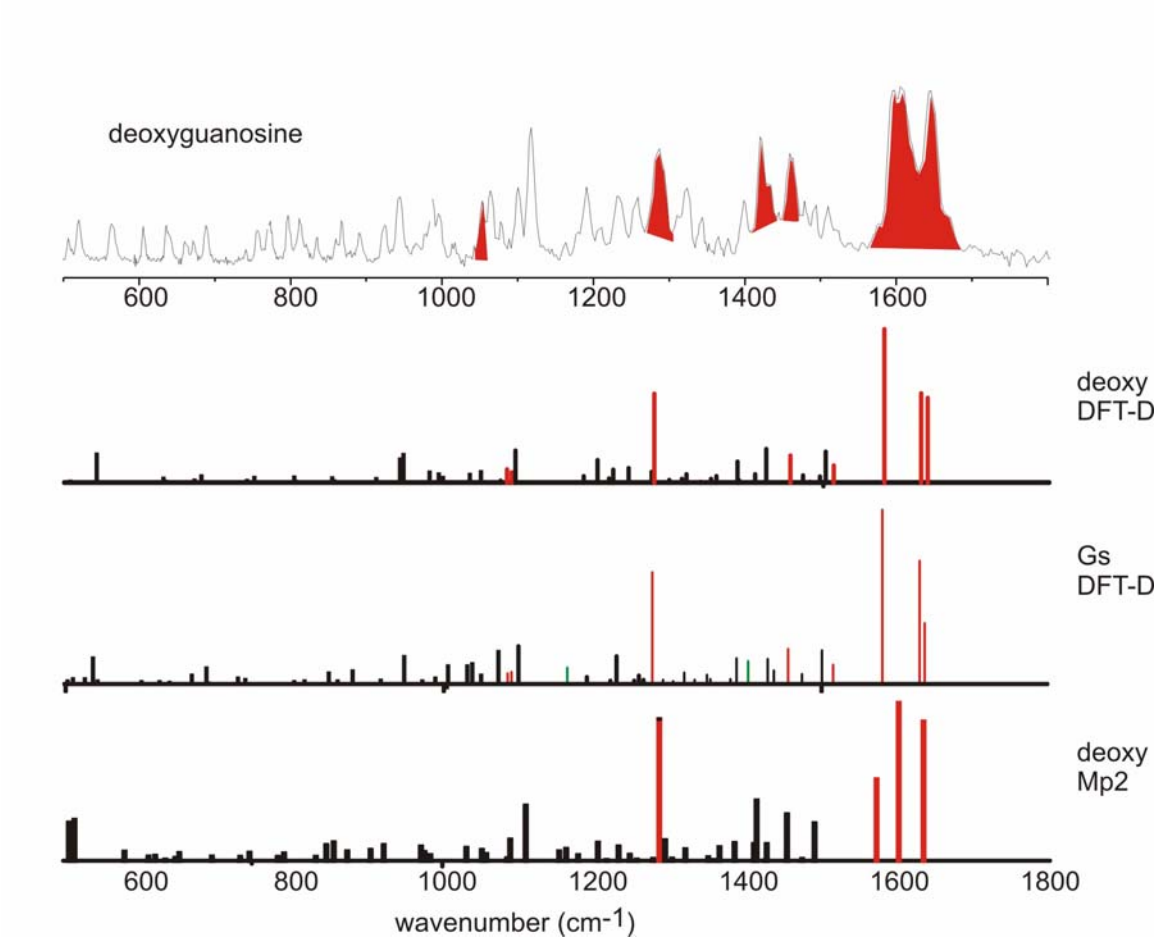
deoxyguanosine
600
800
1000
1200
1400
1600
deoxy
DFT-D
Gs
DFT-D
deoxy
Mp2
600
800
1000
1200
1400
1600
1800
wavenumber (cm-1)

Figure 7